Crystallization of Complexes Characterized with Streaming Potential Measurement

Jian Wang,*,† Wei-xing Ma,† Fu-jun Yin,†,‡ Xing-you Xu,‡,§ Lu-de Lu,‡ Xv-jie Yang,‡ Xin Wang,‡ Yun-long Zang,† and En-wei Lin†

School of Chemical Engineering, Huaihai Institute of Technology, Lianyungang, 222005, China, Materials Chemistry Laboratory, Nanjing University of Science and Technology, Nanjing, 210094, China, and Huaiyin Institute of Technology, Huaian, 223003, China

The streaming potential of supersaturated solutions of $K_3[Fe(CN)_6]$ and $K_4[Fe(CN)_6]$ was determined to characterize crystallization under declining temperature conditions. The value of the streaming potential was related to the oxidation state of the iron atom in the complex, the solubility of the complex, and the starting temperature of crystallization. It was easily influenced by the thermal influence, the polarization of the electrode, the hydrolyzation of the complex, and the rate of the temperature decline. When the temperature dropped to the point where crystal nuclei appeared, the streaming potential reached a minimum. Thereafter, as the number of crystal nuclei increased, some minicrystals grew, and the streaming potential presented a tendency to increase. The higher the starting temperature of the complex saturated solution is, the higher temperature corresponding to the value of the streaming potential minimum is. The temperature of the streaming potential minimum in the $K_3[Fe(CN)_6]$ supersaturated solution is lower than that in the $K_4[Fe(CN)_6]$ supersaturated solution.

1. Introduction

The crystal growth of complexes is a significant step in studying the molecular structure of complexes and material properties. Studying crystallization and investigating phase-transformation characteristics are important to control the crystal quality of complexes. Crystallization is a process where some degree of supersaturation at the initial stage usually exists. While some growth units congregate to form crystal nuclei, they will be covered with beds of complex ions and counterions or complex molecules, one after another, until they reach a definite size. The growth of crystal nuclei can be understood as a course in which complexes in liquid migrate to the surface of crystal nuclei, that is, the interphase of the solution and solid complex steps into liquid phase.[1]

The streaming potential is one of the four electrokinetic phenomena which can be widely used to characterize the charge properties of the liquid−solid interface. This electrokinetic technique has been utilized to measure the zeta potential on the surfaces of glass and amorphous silica in contact with aqueous surfactant solutions and the zeta potential at the muscovite mica basal plane−water interface.[2–4] Natural mica, bare and covered by positively charged latex particles of a micrometer size range, and surfaces modified by particle adsorption were determined by the streaming potential method.[5,6] Furthermore, streaming potential measurements were used to investigate the charge properties on the surface of proteins, polymers, colloidal suspensions, specific crystallographic planes of semisoluble salts, packed capillary columns, and fluid flow in microfabricated microchannels.[7–16] We have also characterized the crystallization of several kinds of typical inorganic salts and binary carboxylic acids from aqueous solution.[17,18] In this research, potassium hexacyanoferrate or yellow prussiate of potash $K_4[Fe(CN)_6]\cdot 3H_2O$ and potassium ferricyanide or red prussiate $K_3[Fe(CN)_6]$ were employed to determine and characterize the crystallization of complexes under declining temperature conditions. Yellow prussiate of potash and red prussiate are two typical iron complexes. The former is a purified complex obtained for the first time by mankind.[19] It was in 1704; the German Diesbach baked and burned grass ash and blood and then leached and crystallized them to obtain the yellow prussiate of potash.

According to the principle of streaming potential, the capillary measurement system was utilized to investigate the behavior of the streaming potential in the crystallization of complexes. The two complexes employed are crystalloid solids. They have the same central atoms, Fe, the same ligand, CN^-, and a similar coordination environment but different oxidation state.

As is known, an electrical double layer can be formed in a glass capillary system full of water.[20–22] When the capillary system is filled with a saturated aqueous solution of $K_3[Fe(CN)_6]$ or $K_4[Fe(CN)_6]$, the positively charged K^+ which is dissociated from $K_3[Fe(CN)_6]$ or $K_4[Fe(CN)_6]$ has a small radius. K^+ is easily hydrated to form a big radius and thick crust ion. Yet another positively charged ion, H^+, is hard to dissociate from water. This weakens the affinity between the K^+ and the negative charge on the surface of the glass. The K^+ is difficult to adsorb on the surface of glass, and it is distributed in the bulk solution, whereas the negatively charged $[Fe(CN)_6]^{4-}$ or $[Fe(CN)_6]^{3-}$ has a bigger radius than OH^- and is hard to hydrate and easy to adsorb on the surface of glass. The adsorption of $[Fe(CN)_6]^{4-}$ or $[Fe(CN)_6]^{3-}$ changes the charge on the surface of the glass. Consequently, it is possible to set up a method which uses the

* Corresponding author. E-mail: wangj@hhit.edu.cn. Tel.: 86-518-85857726. Fax: 86-518-85807426.
† Huaihai Institute of Technology.
‡ Nanjing University of Science and Technology.
§ Huaiyin Institute of Technology.

10.1021/je900098q
Published on Web 03/04/2010

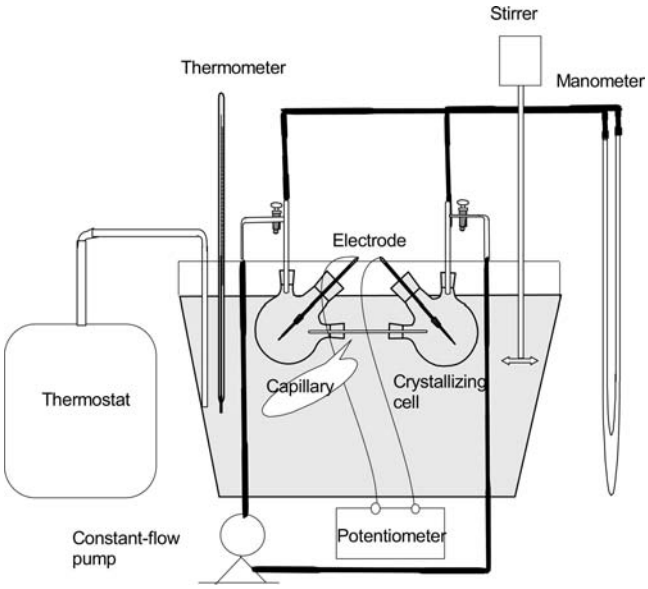

Figure 1. Diagram of streaming potential layout.

streaming potential as a means to characterize the crystal growth of $K_3[Fe(CN)_6]$ or $K_4[Fe(CN)_6]$.

2. Materials and Methods

2.1. Streaming Potential Design. The streaming potential apparatus is as shown in Figure 1. To prevent the electrodes from damage, 0.5 mm diameter platinum wires with a purity of 99.95 % were employed. However, these electrodes are easily influenced by polarization after being used three or four times. So, before using, the platinum wires were soaked in concentrated nitric acid for 1 min and then rinsed with deionized water. Then the electrodes were tested by immersing them in a beaker of 0.1 mol·mL^{-1} KCl solution and connecting them to the electrometer in voltmeter mode. If the bias potential was larger than 0.3 mV or fluctuated by more than 10 %, the electrodes would not meet the requirement of determination. After the measurements, the platinum wires were preserved in deionized water.

2.2. Solutions. Potassium ferrocyanide and potassium ferricyanide were of analytical reagent grade. Water was deionized by an ion-exchange resin and was boiled to drive out air before utilization. The experiments were carried out with freshly prepared solutions. The solubility data of $K_3[Fe(CN)_6]$ and $K_4[Fe(CN)_6]$ were obtained from refs 23 and 24. The relationship between solubility (S, g/100 g of H_2O) of the complex and temperature (t,°C) was determined by Microsoft Excel:

$$S_{K3Fe(CN)6} = 0.732t + 30.66 \qquad (R_2 = 0.9977)$$

$$S_{K4Fe(CN)6} = 0.682t + 14.38 \qquad (R_2 = 0.9996)$$

The saturated solutions under certain temperatures were prepared with a thermostatic bath and volumetric flasks. In the neutral aqueous solution, $K_3[Fe(CN)_6]$ is easily influenced by sunlight. It is able to slightly hydrolyze and gradually decompose to form $K_4[Fe(CN)_6]$. Hence, potassium ferricyanide solutions are not suitable for long-term preservation.

2.3. Temperature Control. Crystallization commonly occurs when the saturated solution of the complex is cooled down. In the experiment, as the initial temperature is different, control of cooling rate is essential for the crystallization process. The temperature was controlled by a freezing thermostat with an outside loop copper pipe coil. The cooling rate in the experiments was adjusted to 0.1 °C·min^{-1}.

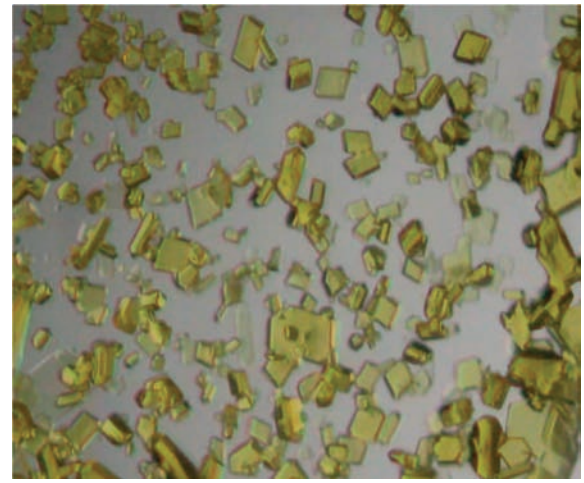

Figure 2. A photograph of $K_3[Fe(CN)_6]$ crystal magnified by a microscope.

2.4. Streaming Potential Operation. Before use of the streaming potential apparatus, the temperature must be consistently maintained for (1.5 to 2) h prior to the crystallization process. The overall setup of this device required a potentiometer (VC890C+TM, Victor) to be connected to the platinum wire electrodes to measure the voltage drop and a manometer to monitor the pressure drop of the flowing liquid. All experimental processes were performed under steady flow conditions. During the measurement procedure, the electrodes were used to monitor the electromotive force generated as the charged ions in the supersaturated solution passed through the charged surface of the glass capillary. These voltage measurements were performed as a function of the pressure gradient across the capillary. This procedure was repeated about twenty times to collect enough data to plot voltage versus the pressure gradient. The rate of the slope from the measured voltage and pressure gradient data was employed to calculate the corresponding streaming potential (ν).

3. Results and Discussion

3.1. Crystallization of $K_3[Fe(CN)_6]$. At a later stage of the temperature reduction process, many tiny block and glassy yellow crystals separate out of the the sanguine supersaturated solution of $K_3[Fe(CN)_6]$. A photograph of these crystals is shown in Figure 2.

Figure 3 shows the variation of the streaming potential ν (mV·Pa^{-1}) with temperature t (°C) for several $K_3[Fe(CN)_6]$ saturated solutions of starting temperatures of (20, 25, 30, and 35) °C. As shown from this figure, the streaming potential in a saturated solution of $K_3[Fe(CN)_6]$ continuously decreases with the decline of temperature in the early stage. When there are formations of the nucleus, the $\nu-t$ curve reaches the lowest point, and the value of the streaming potential will tend to rebound. For a starting temperature of (20 and 25) °C, however, a minimum of streaming potential is not evident. This is because the freezing thermostat is incapable of reducing temperature effectively below 3 °C in the summer. Figure 3 also gives a comparison of four curves from (20, 25, 30, and 35) °C.

For a starting temperature of (30 and 35) °C, there is a point where crystal nuclei emerge. At this point the streaming potential reaches a minimum in the $\nu-t$ curves. After this point, crystal nuclei are increasing with crystallite growth, and the streaming potential gradually rises. The minima of the streaming potential corresponding to starting temperatures of (30 and 35) °C are at points (4.1 °C, $-6.80\cdot10^{-4}$ mV·Pa^{-1}) and (4 °C, $-9.04\cdot10^{-4}$

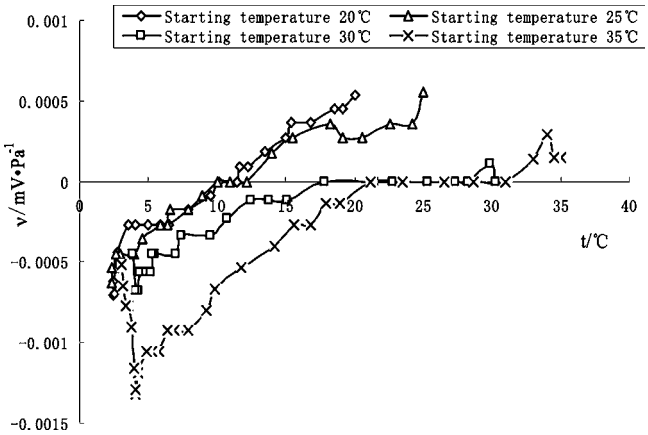

Figure 3. Comparison of ν (mV·Pa^{-1})−t (°C) curves of $K_3[Fe(CN)_6]$ saturated solutions with starting temperatures of (20, 25, 30, and 35) °C.

mV·Pa^{-1}), respectively. By comparing the four curves of starting temperatures at (20, 25, 30, and 35) °C, the results show that the higher starting temperature of the saturated solution is, the lower the $\nu-t$ curve is.

The result can be explained by K^+ and $[Fe(CN)_6]^{3-}$ ions with a certain electric potential in solution constituting the crystal growth unit of $K_3[Fe(CN)_6]$. The basic constitutional unit of the growth unit is $[Fe(CN)_6]^{3-}$. The CN^- ions associate with Fe(III) ions with a coordination bond to form $[Fe(CN)_6]^{3-}$, which has the configuration of a regular octahedron. Along with a change in the degree of supersaturation, the growth unit forms different dimensionality congeries. As these congeries have different quantities of K^+, they have different potentials. When the temperature of solution is below the saturated temperature, the bigger dimensionality basic units couple up with one another and result in a decline of the potential. As soon as crystal nuclei which bear the K^+ growth unit appear, the potential becomes a minimum. Below this point of temperature, the $K_3[Fe(CN)_6]$ concentration decreases, with the declining dimensionality of the growth unit, and K^+ increases, so that the potential ascends.

3.2. Crystallization of $K_4[Fe(CN)_6]$. In the later period of the temperature reduction processs, there are tiny unshaped block and yellowy crystal separated out from the yellow transparent and supersaturated solution of $K_4[Fe(CN)_6]$. These crystals are shown in Figure 4.

A preparatory experiment indicated that, when temperature is constant, the streaming potential of crystallization system is also constant. However, when the temperature declines, the streaming potential changes. Figure 5 gives the variation of the streaming potential ν (mV·Pa^{-1}) with temperature t (°C) for several $K_4[Fe(CN)_6]$ saturated solutions with a starting temperature of (20, 25, 30, and 35) °C. The results are analogous with Figure 3. The streaming potential of $K_4[Fe(CN)_6]$ saturated solutions decreases with a decline of temperature in the previous period. When crystal nuclei appear, the $\nu-t$ curve reaches a minimum point, and the value of the streaming potential tends to rebound. For a starting temperature of (30 and 35) °C, there are obviously double minima of the streaming potential. A possible explanation is that there are two successive crystallizations in two different crystallizing cells. The minima of the streaming potential corresponding to a starting temperature of (20, 25, 30, and 35) °C are at points (6.3 °C, $-2.19\cdot10^{-3}$ mV·Pa^{-1}; 5.1 °C, $-2.07\cdot10^{-3}$ mV·Pa^{-1}), (6.9 °C, $-1.43\cdot10^{-3}$ mV·Pa^{-1}; 4.2 °C, $-1.46\cdot10^{-3}$ mV·Pa^{-1}), (14.1 °C, $-2.66\cdot10^{-3}$ mV·Pa^{-1}; 6.2 °C, $-1.53\cdot10^{-3}$ mV·Pa^{-1}), and (8.0 °C, $-1.31\cdot10^{-3}$ mV·Pa^{-1}; 7.2 °C, $-9.59\cdot10^{-4}$ mV·Pa^{-1}), respectively.

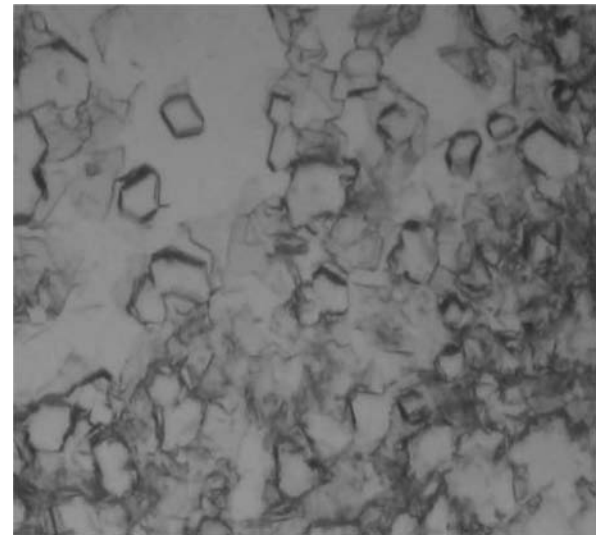

Figure 4. A photograph of $K_4[Fe(CN)_6]$ crystal magnified by a microscope.

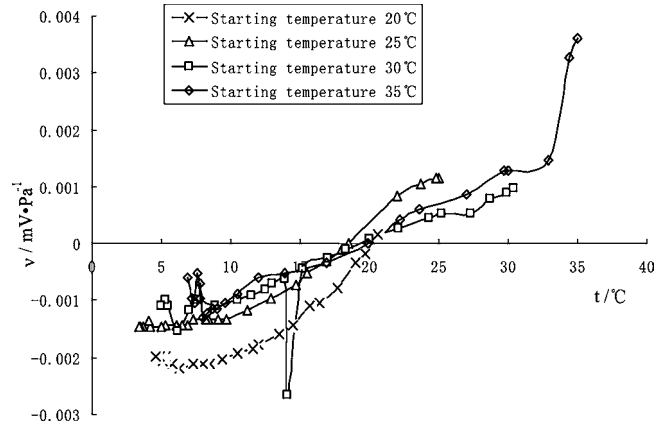

Figure 5. Comparison of ν (mV·Pa^{-1})−t (°C) curves of $K_4[Fe(CN)_6]$ saturated solutions with starting temperatures of (20, 25, 30, and 35) °C.

Figure 5 also gives a comparison of four curves corresponding to a starting temperature of (20, 25, 30, and 35) °C. The results show that the streaming potential continuously decreased with a temperature decline. While crystal nuclei emerge, the streaming potential reaches a minimum. After this point and during crystallite growth, the streaming potential gradually increases.

A possible reason is that the supersaturation degree of $K_4Fe(CN)_6$ solution is increased with descending temperature. Within the area between the substability state and prior to the formation of crystal nuclei, the activity of K^+ ions is reduced because of electrovalent bonds. Because of the integration of $[Fe(CN)_6]^{4-}$ and K^+, the negative charge density of the outlayer $K_4Fe(CN)_6$, which was separated out on the surface of the capillary, becomes lower and causes the streaming potential of the system to decrease with temperature. When crystal nuclei appear in the supersaturated solution, the surface of the crystal nuclei will be negatively charged with a layer of $[Fe(CN)_6]^{4-}$ ions. The dissociated K^+ ions are quite hydrophilic, and they are distributed in the bulk solution. Thus, a electrical double layer is formed on the surface of the crystal nuclei. This will lead to an unstable fluctuation of the streaming potential measurement, and the value of the streaming potential reaches its lowest point. With many stable crystal nuclei appearing, the total surface area will increase with the growth of the crystal, which causes the negative charge density of the crystal surface to decrease. Meanwhile, the concentration of $K_4Fe(CN)_6$ in the

supersaturated solution declines constantly, which increases the activity of K^+ ions and leads to a rising trend of the streaming potential.

3.3. Relationship between the Streaming Potential and the Oxidation State of Iron in the Complex or the Solubility of Complexes and the Influence of Starting Temperature on the Crystallization Process. From the relationship between the streaming potential and the oxidation state of the iron atom in the complexes at a starting temperature of (20, 25, 30, and 35) °C, it shows that the $\nu-t$ curve of $K_3[Fe(CN)_6]$ is higher than that of $K_4[Fe(CN)_6]$ below the temperature corresponding to streaming potential mutation at which the crystal nucleus appears. It seems there is some relativity to the fact that the iron in $K_3[Fe(CN)_6]$ has a higher oxidation state than that in $K_4[Fe(CN)_6]$, and thus the $[Fe(CN)_6]^{3-}$ ion has a lower negative charge than $[Fe(CN)_6]^{4-}$.

A further comparison of the two relevant ν (mV·Pa^{-1})$-t$ (°C) curves between $K_3[Fe(CN)_6]$ and $K_4[Fe(CN)_6]$ under the same starting temperature indicates that the temperature corresponding to the streaming potential minimum of $K_3[Fe(CN)_6]$ is lower than that of $K_4[Fe(CN)_6]$. There is also a point of intersection. Before this point the ν (mV·Pa^{-1})$-t$ (°C) curve of $K_3[Fe(CN)_6]$ is lower than that of $K_4[Fe(CN)_6]$. However, after this point the ν (mV·Pa^{-1})$-t$ (°C) curve of $K_3[Fe(CN)_6]$ will be higher than that of $K_4[Fe(CN)_6]$. This is because $K_3[Fe(CN)_6]$ has a higher solubility and saturated concentration than $K_4[Fe(CN)_6]$, so that the smaller $[Fe(CN)_6]^{3-}$ ion will more easily use electrostatic attraction to form congeries and crystal nuclei than the bigger $[Fe(CN)_6]^{4-}$ ion.

Both Figures 3 and 5 show that the starting temperature of the saturated solution complexes has no obvious correlation to the temperature of streaming potential mutation or minimum at which the crystal nucleus appeared. The results can also be explained by the action of the electrovalent bond. At high temperatures, the saturated solution complexes have a higher solubility and saturated concentration than those at lower temperatures, but the electrovalent bond becomes weaker because of the thermal motion between molecules and the increase of ion activity.

4. Summary

The complexes $K_3[Fe(CN)_6]$ and $K_4[Fe(CN)_6]$ have the same central atom, Fe, and ligand, CN^-, and a similar structure but different oxidation state. In the crystallization process, the value of the streaming potential is related to the oxidation state of the central atom, the solubility of the complexes, and the starting temperature of crystallization. Meantime, it is influenced by the cooling rate, the fluctuation of temperature, the polarization of the electrodes, and the hydrolyzation of the complexes. The relationship between the streaming potential and the temperature of the complex saturated solution has revealed that the streaming potential is reduced in the initial period. When crystal nuclei emerge in the crystallization cell, the value of the streaming potential reaches a minimum. After that, the number of crystal nuclei increase, and minicrystals appear. Then the streaming potential shows an increasing tendency.

Literature Cited

(1) Zhang, K.; Zhang, L. *Science and Technology of Crystal Growth*; Science Press: Bejing, 1997.

(2) Gu, Y.; Li, D. The ζ-Potential of Glass Surface in Contact with Aqueous Solutions. *J. Colloid Interface Sci.* **2000**, *226*, 328–339.

(3) Johnson, S. B.; Drummond, C. J.; Scales, P. J.; Nishimura, S. Comparison of Techniques for Measuring the Electrical Double Layer Properties of Surfaces in Aqueous Solution: Hexadecyltrimethylammonium Bromide Self-Assembly Structures as a Model System. *Langmuir* **1995**, *11*, 2367–2375.

(4) Nishimura, S.; Scales, P. J.; Biggs, S.; Healy, T. W. An Electrokinetic Study of the Adsorption of Dodecyl Ammonium Amine Surfactants at the Muscovite Mica-Water Interface. *Langmuir* **2000**, *16*, 690–694.

(5) Zembala, M.; Adamczyk, Z. Measurements of Streaming Potential for Mica Covered by Colloid Particles. *Langmuir* **2000**, *16*, 1593–1601.

(6) Hayes, R. A. The electrokinetic behaviour of surfaces modified by particle adsorption. *Colloids Surf., A* **1999**, *146*, 89–94.

(7) Elgersma, A. V.; Zsom, R. L. J.; Lyklema, J.; Norde, W. Kinetics of single and competitive protein adsorption studied by reflectometry and streaming potential measurements. *Colloids Surf.* **1992**, *65*, 17–28.

(8) Gittings, M. R.; Saville, D. A. Electrophoretic Behavior of Bare and Polymer-Coated Latices. *Langmuir* **2000**, *16*, 6416–6421.

(9) Churaev, N. V.; Sergeeva, I. P.; Sobolev, V. D. Hydrodynamic Thickness and Deformation of Adsorbed Layers of Polyethylene Oxides. *J. Colloid Interface Sci.* **1995**, *169*, 300–305.

(10) Churaev, N. V.; Sergeeva, I. P.; Zorin, Z. M.; Gasanov, E. K. Adsorption layers of poly(ethylene oxide) on quartz studied using capillary electrokinetics. *Colloids Surf., A* **1993**, *76*, 23–32.

(11) Eremenko, B. V.; Malysheva, M. L.; Rusin, O. D.; Kutsevol, N. V.; Zeltonozskaya, T. B. Adsorption of copolymers of poly(acrylamide) grafted to poly(vinyl alcohol) and its effect on the electrokinetic potential of silica. *Colloids Surf., A* **1995**, *98*, 19–24.

(12) Pagac, E. S.; Prieve, D. C.; Solomentsev, Y.; Tilton, R. D. A Comparison of Polystyrene-Poly(ethylene oxide) Diblock Copolymer and Poly(ethylene oxide) Homopolymer Adsorption from Aqueous Solutions. *Langmuir* **1997**, *13*, 2993–3001.

(13) Michelle, D. R. *Trivacant Heteropolytungstates as Building Blocks for new polyoxometalates and Catalytic Materials*; UMI Company: Ann Arbor, MI, 1999; 3123359.

(14) Keqing, F. *Interfacial Chemistry in the Fluorite and Calcite Flotation Systems*; UMI Company: Ann Arbor, 2004; 3137301.

(15) Isabelle, M. G. *Capillary Electrochromatography of Peptides and Proteins on Novel Porous Monolithic Packings*; UMI Company: Ann Arbor, MI, 2001; 3030778.

(16) Lawrence, K. *Study of the Fluid Flow in Microfabricated Microchannels*; UMI Company: Ann Arbor, MI, 1998; 9922916.

(17) Wang, J.; Xu, X. Y.; Lu, L. D.; Yang, X. J.; Ma, W. X.; Cui, X. N. Crystallization of binary carboxylic acid with streaming potential measurement. *Surf. Interface Anal.* **2007**, *39*, 482–486.

(18) Wang, J.; Zhou, H. Y.; Wang, M. Y.; Li, S. Z.; Ma, W. X.; Xu, X. Y.; Jiang, P. Q.; Wang, B. G.; Shen, G. Q. Descent Temperature Process of Crystallization Studied by the Streaming Potential. *J. Synth. Cryst.* **2005**, *34*, 557–561.

(19) Zhao, K. H.; Chen, X. W. *A Brief History of Chemistry*; Science Press: Beijing, 1980.

(20) Matthijs, W.; Haartsen, W. D.; Toksîz, M. N. Dynamic streaming currents from seismic point sources in homogeneous poroelastic media. *Geophys. J. Int.* **1998**, *132*, 256–274.

(21) Miller, J. D.; Keqing, F. The surface charge of fluorite in the absence of surface carbonation. *Colloids Surf., A* **2004**, *238*, 91–97.

(22) Alan, D. B. *Colloidal and Interfacial Phenomena in Polymer/Surfactant Mixtures*; UMI Company: Ann Arbor, MI, 2001; 3040435.

(23) Kuang, S. L. *Technical Encyclopedia of Chemical Engineer*; Chemical Industry Press: Beijing, 2002.

(24) Peter, E. L.; Perry, R. H. *PERRY Handbook of Chemical Engineering*, 6th ed.; McGraw Hill, Inc.: New York, 1992.

Received for review January 24, 2009. Accepted February 20, 2010. The authors sincerely acknowledge the Natural Science Research Project of Jiangsu Higher Education (08KJB150002) and the Project of Six Types Major Talent of Jiangsu Province (07-A-024), Science and Technology Key Projects of Lianyungang City (CG0803-2), Doctoral scientific research project (KQ09006) and nature science projects (Z2009018), and the partnership of Huaihai Institute of Technology.

JE900098Q